Multimedia Tools and Applications
https://doi.org/10.1007/s11042-024-19207-7

No reference retinal image quality assessment using support vector machine classifier in wavelet domain

Sima Sahu[1] · Amit Kumar Singh[2] · Nishita Priyadarshini[3]

Received: 19 February 2024 / Revised: 21 March 2024 / Accepted: 5 April 2024
© The Author(s), under exclusive licence to Springer Science+Business Media, LLC, part of Springer Nature 2024

Abstract
The automatic retinal screening system (ARSS) is a valuable computer-aided diagnosis tool for healthcare providers and public health initiatives. The ARSS facilitates mass retinal screenings that analyse retinal images and detect early signs of vision-threatening retinal diseases. The degradation in retinal image's naturalness causes imprecise diagnosis. This paper proposed a quality assessment method that is suitable for ARSS and is important for closing care gaps and reducing healthcare costs in the field of healthcare. A no-reference (NR) quality assessment method utilizing natural scene statistics (NSS) and the multi-resolution approach is developed to detect retinal image quality. Image quality classification is performed combining NSS features and statistical featurenns of retinal image. A support vector machine classifier is used to map the retinal image features and find image quality. The proposed method is compared with existing NR image quality assessment methods. The results show that the proposed method has improved accuracy, recall, precision and F-measure values of 3.42%, 3.66%, 1.63% and 2.66%, respectively, over the competing methods, demonstrating its suitability for ARSS.

Keywords Natural Scene Statistics (NSS) · Support Vector Machine (SVM) · No-Reference (NR) quality assessment · Wavelet transform

✉ Amit Kumar Singh
amit.singh@nitp.ac.in

Sima Sahu
simahal@mrec.ac.in

Nishita Priyadarshini
nishitapriya2019@gmail.com

[1] Department of ECE, Malla Reddy Engineering College (Autonomous), Maisammaguda, Hyderabad, Telangana, India

[2] Department of Computer Science & Engineering, National Institute of Technology Patna, Patna, India

[3] AIIMS Bibinagar, Hyderabad, Telangana, India

Published online: 19 April 2024

1 Introduction

Retinal disorder in different components of the eye, such as the retina, optic nerve, iris, lens and pupil, leads to visual impairment and vision loss [1]. The leading causes of blindness are glaucoma, diabetic retinopathy (DR), age-related macular degeneration (AMD) and cataracts. The primary cause of blindness is AMD, which damages the macula and results in central vision loss. The second leading cause of blindness is glaucoma, which affects the optic nerve and results in peripheral vision loss. Retinal damage is irreversible. By 2030, the global DR patient population is expected to reach around 439 million. Worldwide, 2.2 billion people suffer from visual impairment and approximately 1 billion people suffer from retinal disorder, which may possibly be avoided. In India, 25% of people over the age of 50 are visually impaired. Among them, blindness prevalence is at 1.99%. Visual impairment and blindness due to preventable causes is at 97.4% and 92.9%, respectively [2]. A premature retinal disease diagnosis is essential to stop the disease's progression. As early signs of retinal diseases are absent, detecting retinal disease is highly essential. In the case of mass screening, manual detection is not always effective due to the requirement of an expert and the length of time the procedure takes. Automated retinal diagnosis overcomes the above-mentioned challenges. The automatic retinal screening system (ARSS) facilitates early retinal disease diagnosis [1]. A reliable ARSS requires accurate diagnosis and is strongly reliant on retinal image quality. Factors responsible for retinal image quality degradation are loss of focus, patient movement and a non-dilated pupil. Sudden vision changes, refractive error and eye strain cause loss of focus. Figure 1 shows the different causes of fundus image quality degradation during image acquisition. The image degradation results change in pathological structures of retinal image. The main causes of degradation are loss of focus, patient eye motion during scanning and non-detailed pupil. Factors responsible for capturing quality fundus image are: resolution, sensor quality, proper spacing between eye and camera, contrast and flash adjustment.

Fundus image quality can be evaluated by the following [2]:

1. Human perception
2. Full Reference Image Quality Assessment (FR-IQA)
3. No Reference Image Quality Assessment (NR-IQA)

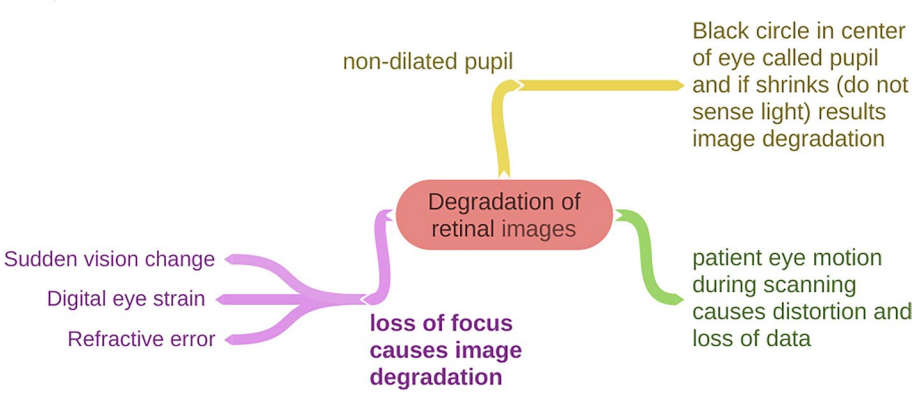

Fig. 1 Factors responsible for fundus retinal image quality degradation

Human perception is performed through the visual inspection of a retinal image. Visual inspection is subjective commonly used for quality assessment. Perceptual quality is evaluated based on colour accuracy, sharpness and contrast. This process is not very effective because of potential bias, differences in perception and inconsistencies among observers.

The full-reference image quality assessment (FR-IQA) method uses a reference image to quantify the image's quality by differentiating it from the distorted image [3]. Various attributes are used for comparison, such as structural similarity and statistical features between the reference and distorted images. The most significant limitation of the FR-IQA is its dependency on accessing the reference image. An ideal image version is difficult to obtain, so the no-reference image quality assessment (NR-IQA) method is preferred for quality assessment. The NR-IQA method quantifies image quality by exploiting degraded image features. Based on information contained within it, this method uses statistical models to assess image quality. The NR-IQA method's design can be challenging because the image features may be captured inaccurately. The NR-IQA method has an important application in areas where a reference image is unavailable especially medical images.

The proposed work evaluates retinal image quality without the knowledge of a distortion type or reference image. Natural scene statistics-based (NSS-based) retinal image features and multi-resolution based image features are extracted to find the image quality. Wavelet coefficients characterise the heavy-tailed distribution [4]. This multi-resolution based wavelet transform characteristic is used to extract distribution parameters. Traditional methods used raw image pixels to extract features in thespatial domain.

The principal contributions and novelty of the proposed research include:

- Wavelet-based methods overcome the limitations of structure-based methods by extracting retinal features from sub-bands of subsequent wavelet levels.
- The feature-based method using wavelet transform is computationally inexpensive. It has multi-resolution features and, thus, maintains consistent performance in different resolutions [5].
- This research supports the ARSS and has considerable evidence for the global effort against visual impairment caused by retinal diseases.

The organization of this paper is as follows: relevant literature is discussed in Section 2. Proposed research methodology is discussed in Section 3. The findings and result analysis is performed in Section 4 and observations and overall implication of the proposed work is discussed in conclusion, Section 5.

2 Related work

The NR-IQA methods define image quality and reject unsuitable retinal images for further diagnosis. Several NR-IQA techniques are implemented in literature considering retinal and non-retinal images [6–8]. Distortion, such as noise, blurs and compression is the main cause of retinal image degradation and must be considered in quality assessment methods. Figure 2 shows the classification of IQA techniques for Fundus images.

Subjective assessment technique involves visual inspection and objective assessment involves assessment through mathematical calculations. Subjective assessment is a time-consuming and expensive method. This assessment result heavily depends on the observer's emotional and physical condition. It is unsuitable for real-time application. Subjective

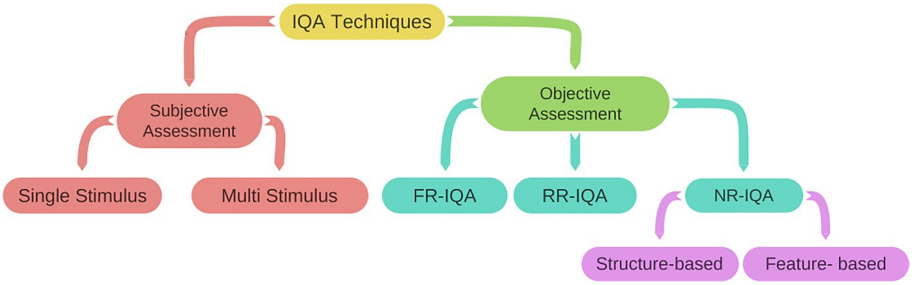

Fig. 2 Classification of Fundus IQA techniques

assessment can be further divided as single stimulus and multi stimulus method. The single-stimulus method involves displaying an image for a fixed duration of time, while the multi-stimulus method involves randomly displaying a test image to the observer.

Objective assessment method uses mathematical models to automatically and accurately predict image quality.Objective assessment method can be classified as FR-IQA, RR-IQA and NR-IQA based on the availability of reference or true image.The FR-IQA technique is used in the presence of an undistorted original image. In the reduced-reference image quality assessment (RR-IQA) technique, a part of thedistorted image is compared.In the absence of original or undistorted image, theNR-IQA techniqueis preferred that involves extracting features from an image to assess quality. This technique can be classified as structure-based and feature-based. In a structure-based technique, retinal image quality is determined from segmented structure. The clustering method [9] and blood vessel structure [10] are examples of structure-based methods. A structure-based method heavily depends on the performance of structure segmentation [13]. The result depends on an image's structural features and neglects contextual information. A structure based NR quality assessment method was proposed by Chow et al. [7] formagnetic resonance (MR) images. Luminance coefficients were used as image feature to find image quality with the hypothesis that their distribution vary with distortions. This method achieved high association with human estimation for structural images, but failed for functional images.A further improvement in this method was proposed by Ou et al. [8]. The authors proposed a blind IQA method to find the quality in non-retinal images. Transform domain features are combined with statistical features to predict the image quality accurately. The authors considered Gaussian distribution shape parameters and image entropy features with the luminance coefficient parameters. This method is not suitable for images with acomplex structure because of the time complexity in extracting features. A segmentation based IQA method for retinal image was developed by Nugroho et al. [16].The authors used blood vessel intensities for accessing quality. Their method was effectual for fixed dimension of blood vessels and not suitable for smaller or larger size blood vessels. The segmentation methods analyze the pathological information in retinal images. The quality assessment result depends on the segmentation results of structural data. Segmentation IQA methods are not reliable in the presence of noise.

IQA methods are further enhanced by introducing feature based methods. Feature-based methods extract and analyse various image features to predict the retinal image's quality. Features such as colour, illumination, focus and contrast are used in feature-based RIQA techniques to assess image quality [13, 21]. Feature based IQA methods are based on structural analysis and generic statistical features of retinal images. Feature based methods

implement machine learning to improve efficiency and accuracy. A NR-IQA method was proposed by Fu et al. [13] that used colour space information as features. The authors designed a colour space fusion network using parallel CNN. Their proposed method achieved high accuracy but computationally expensive due to rapid increase in scale of parameters. One of the most important challenges in machine learning based model is selection of efficient datasets for classification. Table 1 presents overview of existing techniques in NR-IQA considering non retinal and retinal images summarizing techniques, datasets, features analyzed and key results.

Existing feature based IQA methods have several challenges like:

- Image features to be considered for the evaluation of quality.
- NSS features are not enough to precisely assess the image quality.
- IQA technique should be able to handle all possible types of distortions.

Existing methods rely on NSS features for assessing the image quality likely: blood vessel structure, morphological changes in macula and optic disc, distortions in colour and contrast and blur during image acquisition. The classification accuracy of the existing methods was not satisfactory as they failed to consider the statistical features of image and noise concepts. The proposed research overcomes the above-mentioned gaps by handling widely diverse image distortions. This paper considers both spatial and wavelet domain features to construct a model that considers both structural, statistical features and inherent noise to assess image quality accurately. Feature vectors are built with regard to both domains. The proposed methodology's effectiveness was assessed through extensive experimentation.

3 Proposed work

In this section, a new NR-IQA framework is presented based on a support vector machine (SVM) classifier in a multi-resolution approach. This section also covers the wavelet decomposition method, the extraction of features in the wavelet domain, NSS features extraction and the SVM classifier.Flow chart of the proposed No-Reference RIQA is summarized in Fig. 3. First, feature vectors were extracted from a fundus retinal image in the wavelet domain environment. Signal and noise variance and location parameter features were evaluated by statistically modeling the wavelet coefficients. Sharpness, contrast and spatial correlation features were calculated by analysing sub-band coefficients. Next, all feature vectors were processed through an SVM to be classified as *superior* (good) or *eliminate* (bad) quality.The features employed in the proposed method are listed in Table 2.

3.1 Wavelet feature extraction

Wavelet transform is a multi-resolution approach, which results in four sub-bands: approximation, horizontal, vertical and diagonal. Wavelet transform composed of high-pass and low-pass filters has the advantages of both frequency and time localisation. Approximation sub-band (LL) contains a smoothed description of the original image. Horizontal (LH), vertical (HL) and diagonal sub-bands (HH) contain high-frequency information, which defines the detailed edge information. Finer edge details are obtained by further wavelet decomposition of the approximation sub-band. Wavelet transform separates high frequency components that give

Table 1 Comparison of state-of-the-art studies in NR-IQA

Methods	Dataset	Features implemented	Technique	Key results
Non-retinal image as input				
Modified BRISQUE [7]	Osirix DICOM Viewer MRI database	Luminance Coefficients	SVR model	PLCC = 0.901, SROCC = 0.890 RMSE = 2.985
NBIQA [8]	LIVE-IQA &LIVE-C	Spatial and DCT domain features	Refined NSS model using SVM tool	Mean SROCC:LIVE IQA = 0.959, LIVE-C = 0.63 ± 0.03Mean PLCC: LIVE-C = 0.64 ± 0.03
Retinal image as input				
Nugroho et al. [16]	HEI-MED	Intensities of blood vessels and non-blood vessels	Segmentation of Blood vessels	Sensitivity = 0.97619, Specificity = 0.8, Accuracy = 0.89362
Hamid et al. [21]	DRIMDB & HRF	Wavelet level, sharpness and Contrast	Wavelet decomposition sub-band feature extraction	AUC = 1(High resolution dataset) AUC = 0.985 (Low resolution Dataset)
Zago et al. [19]	DRIMDB & ELSA-Brasil	Generic features	CNN using fine tuning procedure	AUC: DRIMDB = 99.98% ELSA Brasil = 98.56%
Fu et al. [13]	EyeQ	Color, illumination, focus and contrast	Multiple color space fusion network	Accuracy = 0.9175, Precision = 0.8645 Recall = 0.8497, F-measure = 0.8551
Raj et al. [12]	DRIMDB &EyeQ	Structural properties such as visibility of optic disc, Macula and blood vessels and generic features such as blur, color and contrast	Multivariate Regression based CNN	SROCC = 0.942, PLCC = 0.954, KCC = 0.853 Accuracy DRIMDB = 98.96% EyeQ = 88.43%
Abdel-Hamid et al. [20]	DR1,DRIMDB &MESSIDOR	Generic features like edges and colors	Transfer learning based on modified VGG16 network	Accuracy = 99% to 100%
Yulianti et al. [15]	Fundus retinal image captured by Fundus camera	Blood vessel contrast, histogram features and Gray-Level Co-occurrence Matrices (GLCM)	Clustering with K-Nearest Neighbour (KNN) method	Accuracy = 72.41% Specificity = 77.36%

Table 1 (continued)

Methods	Dataset	Features implemented	Technique	Key results
Xu et al. [11]	Kaggle	Vessel and optic disc region structures	Deep CNN	Accuracy = 0.8897 Precision = 0.8748 Recall = 0.8721 F-score = 0.8723
Wang et al. [14]	LOCAL2, DRIMDB	Multi-channel sensation, contrast and blur from retinal fundus image	Human Visual System (HVS) and Support Vector Machine (SVM) methodology	Sensitivity = 87.45%, Specificity = 91.66%, AUC = 0.9452
Kohler et al. [17]	DRIVE	Blur were used as image features to find the spatially weighted quality score	Correlation Analysis	Spearman rank correlation: For PSNR = 0.89, SSIM = 0.91
Abdel-Hamid et al. [18]	DRIMDB DR1 DR2 HRF MESSIDOR	Image illumination, homogeneity and sharpness in wavelet domain	Wavelet Transform and SVM classifier with Radial Basis Function (RBF) kernel	AUC = 0.927
König et al. [25]	Images from Vienna Reading Center (VRC)	Contrast, Focus, Illumination, Shadow, Reflection, Contrast, Focus, noise	Deep Learning	Colour fundus: F1-score = 0.907, AUC = 0.963 Accuracy = 0.930 Fluorescein Angiography: F1-score = 0.822, AUC = 0.918, Accuracy = 0.895

Abbreviation: *PLCC* Pearson's Linear Correlation Coefficient; *SROCC* Spearman's Rank Ordered Correlation Coefficient; *RMSE* Root Mean Square Error; *AUC* Area under the receiving operator characteristic curve; *KCC* Kendall rank-order correlation coefficient; *SSIM* Structural Similarity; *PSNR* Peak-Signal-to-Noise-Ratio

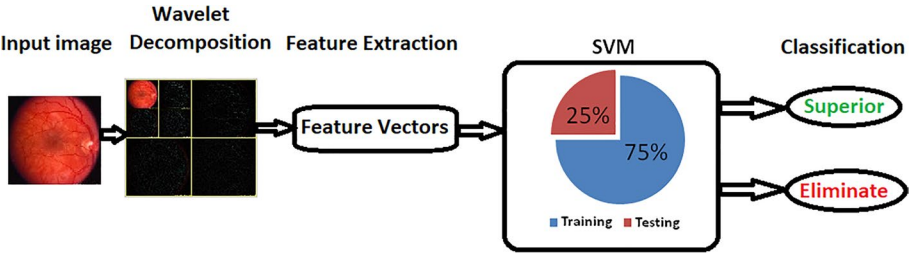

Fig. 3 Flow chart of proposed RIQA technique

noise distribution information in image. Figure 4 shows the first and second level sub-bands of retinal fundus image.

3.2 Sharpness and contrast measurement

Sharpness of an image can be obtained through high-frequency information. The diagonal sub-band contains the high-frequency components. In this paper, Wavelet Shannon entropy [21] metric is used to find the sharpness of retinal image and is defined as:

$$Wavelet\ Shannon\ Entropy = \frac{1}{H+V}(Horizontal\ subband\ enropy + Vertical\ Subband\ Entropy) \quad (1)$$

$$\begin{gathered} subband\ enropy = -\sum_{i=1}^{N} |W_i|^2 log|W_i|^2 \\ W_i = Wavelet\ Subband\ coefficients \end{gathered} \quad (2)$$

H and V are the total number of coefficients in horizontal and vertical sub-bands respectively. Sub-band Entropy is defined both for horizontal and vertical Sub-bands.

Contrast [21] in the image is defined as the ratio of high frequency to its low frequency. Contrast is defined as:

$$Contrast = \left[\frac{\frac{1}{H+V}\left(\sum_{i=1}^{H} |W_i| + \sum_{i=1}^{V} |W_i|\right)}{\sum_{i=1}^{A} |W_i|} \right] \quad (3)$$

A is the total number of coefficients in Approximation subband.

3.3 Signal and noise variance and location parameter of wavelet distribution

A suitable, heavy-tailed distribution, the Cauchy probability density function (PDF) was implemented in this study to model wavelet coefficients and find thesignal distribution's variance and location parameter. Horizontal, vertical and approximation sub-bands were modelled using theCauchy PDF. Inter-scale dependency between wavelet coefficients was utilised to extract the parameters of the Cauchy distribution [22]. Cauchy PDF $f_x(X)$ with location parameter m(real) and scale parameter b is defined as:

Table 2 List of features used to find IQA

Feature	Description	Computational process
$F_1 - F_{12}$	Sharpness and Contrast measurement	Wavelet Shannon Entropy and analyzing the sub-band coefficients
$F_{13} - F_{21}$	Variance of wavelet distribution in Approximation, Horizontal and Vertical sub-bands in all scales	Wavelet sub-bands modeling using heavy tail distribution
$F_{22} - F_{30}$	location parameter of wavelet distribution in Approximation, Horizontal and Vertical sub-bands in all scales	Wavelet sub-band modeling using heavy tail distribution
$F_{31} - F_{33}$	Noise variance in diagonal sub-band	Diagonal sub-bands modeling using Gaussian PDF
$F_{34} - F_{63}$	Spatial correlation across all scale sub-bands	Fitting the correlation function using 3rd order polynomial function

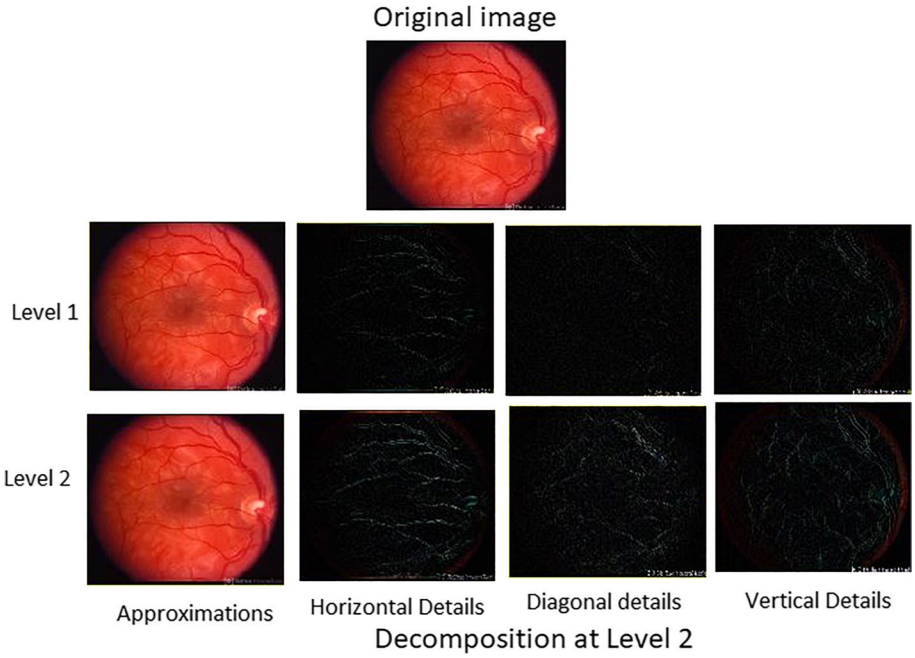

Fig. 4 Wavelet decomposition of retinal Fundus image

$$f_x(X) = \left(\frac{1}{\pi}\right)\left(\frac{b}{(X-m)^2 + b^2}\right) \tag{4}$$

As the distributions of wavelet coefficient in HL, LH and HH sub-bands are heavy tailed in structure, the authors have chosen Cauchy PDF to find location parameter by model these sub-bands. Wavelet coefficient distribution for different types of images is shown in Fig. 5. It can be seen that wavelet coefficients distribution in original image differs noisy image and, blurred and noisy image.

Gaussian PDF is used for modeling diagonal sub-bands and extract noise variance using the following equation:

$$\widehat{\sigma}_n^2 = \left(\frac{\text{Median}(\textit{Diagonal subband})}{0.6745}\right)^2 \tag{5}$$

Figure 6 shows the diagonal sub-band for retinal image for different image quality. From the figure it is found that sharp image has more retinal information rather than blurred images.

3.4 Spatial correlation

An image's spatial structure defines smoothness and can be used to evaluate the quality factor. The correlation between spatial structures in the wavelet sub-band is used to find

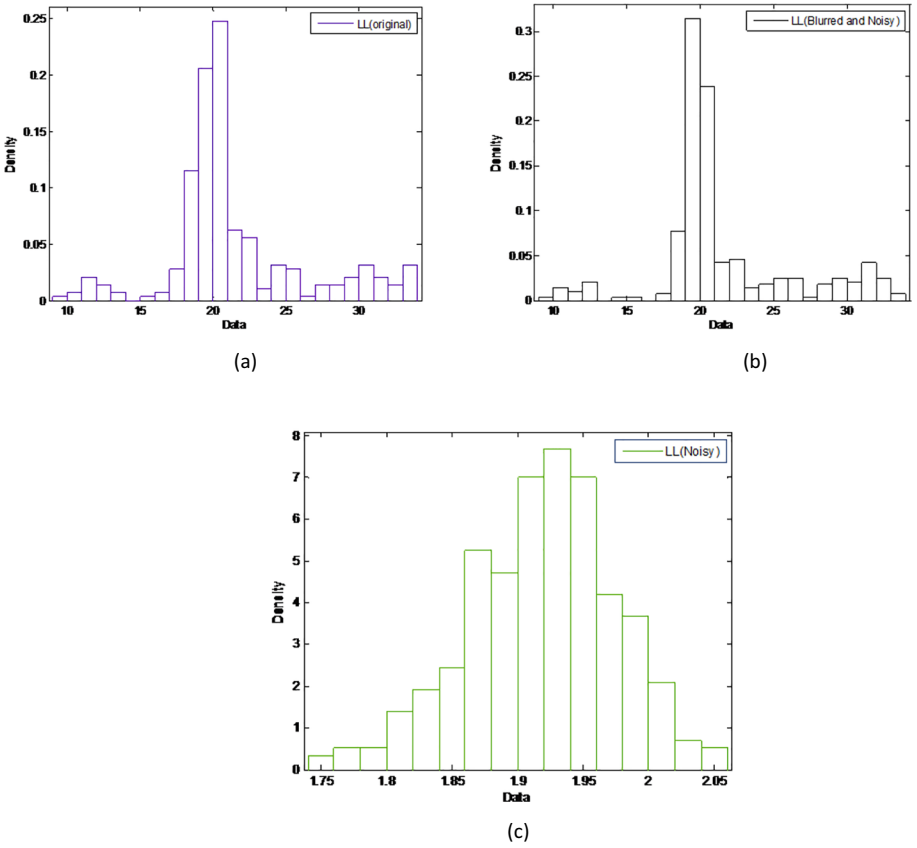

Fig. 5 Wavelet coefficient distribution for different quality images (**a**) Original image (**b**) Blurred and Noisy image (**c**) Noisy image

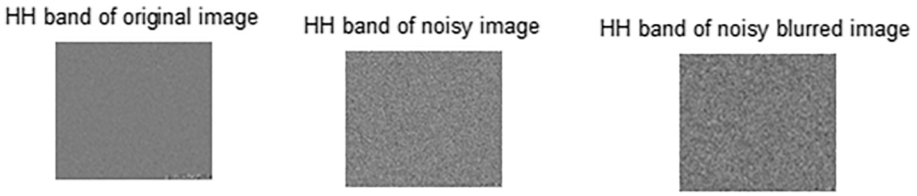

Fig. 6 Diagonal sub-bands of retinal image for different image quality

smoothness. Included in the steps for determining structural correlation is the calculation of joint empirical distribution $f_{x1,y1}(X1, Y1)$ between the coefficients and neighbourhoods at distances $d \in \{1, 2, \ldots \ldots 25\}$. Next correlation between the variables $X1, Y1$ is calculated using the following Eq. (6).

$$\rho_d = \frac{E_{x1y1}(X1, Y1)\left[X1 - E_{x1}(X1)\right]^T \left(Y1 - E_{y1}(Y1)\right)}{\sigma_{x1}\sigma_{Y1}} \tag{6}$$

where E defines expectation operator and σ_{X1}, σ_{Y1} defines variances of X1 and Y1 vectors respectively. Then ρ_d is parameterized by fitting a 3rd order polynomial and coefficient of the polynomial is calculated.

3.5 Support vector machine classifier

The feature classification problem is solved by utilizing a support vector machine (SVM) classifier for classifying retinal fundus image as "superior or "Eliminate" [23].

Let v_i vectors for i = 1,2,3….N are selected from a feature space V. The target values for each feature vector are associated as $Z_i \in \{-1, +1\}$. A hyperplane that maximizes the separating margin between feature vectors is developed for linearly separable features that divide the features in two classes. A kernel method is developed in nonlinear case for separating two classes.

Let $\emptyset(v)$ is the high dimension feature space. Class membership can be found by the function $sign[f(v)]$. $f(v)$ is a function distinguishes two classes and related to hyperplane in transformed space. $f(v)$ can be expressed as:

$$f(v) = w^T \emptyset(v) + b \tag{7}$$

w is the weight vector and b is the bias of the optimal hyper plain. The main aim is to minimize the error and maximize the margin and it can be achieved by minimizing the cost function. The cost function is defined as:

$$\psi(w, \xi) = \frac{1}{2}\|w\|^2 + C\sum_{i=1}^{N} \xi_i \tag{8}$$

The cost function can be minimized by following the constraint:

$$Z_i\left(w\emptyset\left(v_i\right) + b\right) \geq 1 - \xi_i \text{ For } i - 1, 2, 3 \ldots .N \tag{9}$$

The shape of the function $f(v)$ is controlled by the regularization parameter C and its value is set to 1. ξ_i handles non-separable features is called slack variable.

The optimization problem is further redesigned using a kernel function $K(v_i, v_j)$ and Lagrange multiplier $\beta = [\beta_1, \beta_2, \beta_3, \ldots \ldots \ldots \ldots \ldots .\beta_N]$ and is defined as:

$\max_{\beta} \sum_{i=1}^{N} \beta_i - \frac{1}{2}\sum_{i,j=1}^{N} \beta_i\beta_j Z_i Z_j K(v_i, v_j)$ under the constraint $\beta_i \geq 0 and \sum_{i=1}^{N} \beta_i Z_i = 0$. The proposed method utilizes radial Gaussian basis kernel function defined as:

$$K\left(v_i, v_j\right) = exp\left(\frac{-1}{2\sigma^2\|v - {v_i}^2\|^2}\right) \tag{10}$$

where $\sigma = 1$ defines the width of Gaussian kernel.

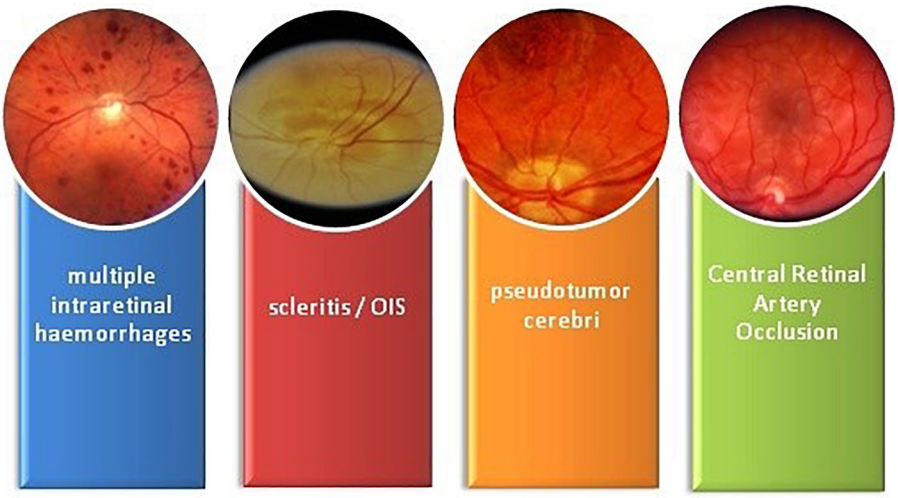

Fig. 7 Samples of Fundus retinal images with abnormalities from Retinal Image Bank [24] database

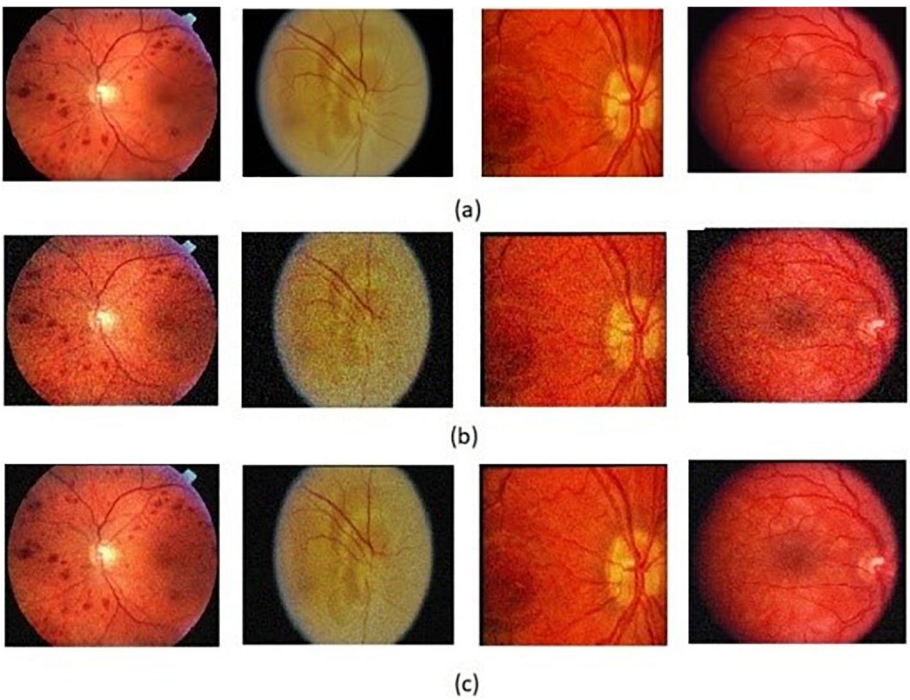

Fig. 8 Retinal fundus images with different quality (**a**) Original image (**b**) noisy image (**c**) Blurred and noisy image

Table 3 Performance evaluation metrics of classifier

Metrics	Procedure
Accuracy	$\frac{TP+TN}{TP+TN+FP+FN}$
Recall/Sensitivity	$\frac{TP}{TP+FN}$
Precision	$\frac{TP}{FP+TP}$
F-measure	$\frac{(2\times TP)}{(2\times TP)+FP+FN}$

Abbreviation: *TP* stands for True positive; *TN* stands for True negative, *FP* stands for false positive and *FN* stands for False negative

Table 4 Performance comparison of proposed and state-of-the-art methods

Input	Methods	Accuracy (%)	Recall (%)	Precision (%)	F-measure (%)
Non-retinal images	Modified BRISQUE [7]	83.66	83.41	91.93	87.46
	NBIQA [8]	86.66	85.92	93.44	89.52
Retinal Fundus image	Nugroho et al. [16]	88.00	87.50	94.08	90.67
	Hamid et al. [21]	88.33	87.00	95.08	90.86
	Zago et al. [19]	90.00	88.32	96.13	92.05
	Fu et al. [13]	92.66	92.50	96.35	94.38
	Raj et al. [12]	93.33	93.59	96.44	94.99
	Abdel-Hamid et al. [20]	94.00	93.96	96.89	95.40
	Yulianti et al. [15]	89.00	88.38	94.59	91.37
	Xu et al. [11]	91.33	90.90	95.74	93.25
	Proposed method	97.33	97.53	98.50	98.01

4 Experimental results

This section discusses the performance results of the proposed technique against the NR-IQA literature methods. The proposed method was validated by 1,500 fundus retinal images collected from the Retina Image Bank [24]. Figure 7 shows samples of fundus retinal images with abnormalities from the Retina Image Bank. Figure 8 shows fundus images of different qualities. The first row shows good quality images, the second row shows noisy images and the third row shows noisy and blurred images. The image data is divided into two sets, training and testing in a 4:1ratio. The feature vector values assessed from the fundus retinal images were used to train the SVM classifier in two classes: superior and eliminate. All the simulation work was performed in a MATLAB environment. Comparison results were discussed through evaluation metrics such as average accuracy, recall, precision and F-measure.

4.1 Performance evaluation metrics

The classifier is desired with high classification accuracy and low misclassification errors. A binary classifier was implemented in this study, and the evaluation of the classifier was

performed through metrics such as average accuracy, recall, precision and F-measure. The evaluation metrics are discussed in Table 3.

4.2 Comparison of proposed method with state-of-the-art methods

The advancement of the proposed method was evaluated by comparing it with state-of-the-art methods, as discussed in Table 4. The proposed method is compared with existing non-retinal and retinal quality assessment methods, each employing distinct methodology. Non-retinal methods are modified-BRISQUE [7] and NBIQA [8] and retinal methods included several studies [11–13, 15, 16, 19–21]. The non-retinal methods were simulated for retinal images and the regression method replaced classification. Methods such as [16, 21] are based on hand-crafted features and methods [11–13, 15, 19, 20], utilise deep features. From Table 4, it is observed that:

- Higher accuracy is achieved by deep feature-based methods than by hand-crafted feature-based methods. The means that hand-crafted features are possibly less effective than deep features.
- Non-retinal quality assessment methods, modified-BRISQUE [7] and NBIQA [8] are less effective than retinal quality assessment methods.
- The proposed method shows more favourable performance metrics (97.33% against accuracy, 97.53% against recall, 98.50% against precision and 98.01% against F-measure) than existing NR-IQA methods. The retinal image suitability required for ARSS should be free from all types of distortion. The proposed method considered NSS features along with noise and signal statistical features in multi-resolution environments that precisely classify and differentiate good images from bad images. The performance results demonstrate the potential of the proposed method to enhance retinal disease diagnoses.

Table 5 Comparison of outcomes of classifiers

NRIQA techniques	Classifier	TP	TN	FP	FN
Structure and generic based NRIQA					
Modified BRISQUE [7]	SVM	171	15	34	80
Xu et al. [11]	CNN	180	8	18	94
Raj et al. [12]	CNN	190	7	13	90
Yulianti et al. [15]	KNN	175	10	23	92
Nugroho et al. [16]	KNN	175	11	25	89
Feature based NRIQA					
NBIQA[8]	SVM	171	12	28	89
Fu et al. [13]	CNN	185	7	15	93
Zago et al. [19]	CNN	174	7	23	96
Abdel-Hamid et al. [20]	SVM	187	6	12	95
Hamid et al. [21]	KNN	174	9	26	91
Structure and statistical features based NRIQA					
Proposed method	SVM	198	3	5	94

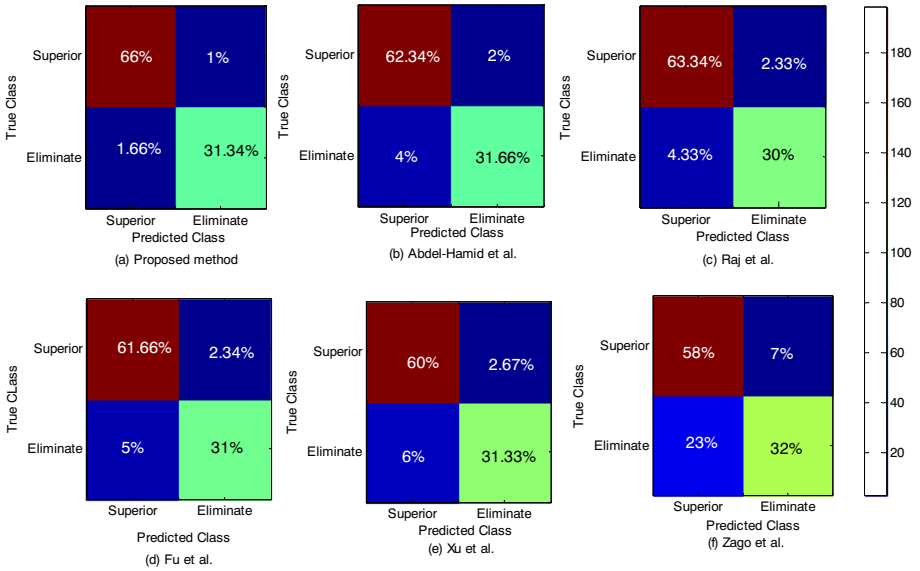

Fig. 9 Confusion matrix for different methods

A comprehensive comparison between the outcomes of classifier is discussed in Table 5. It is observed that the prediction rate accuracy of the classifiers not only depends on the efficiency of the classifier but the efficient dataset over which it works. The SVM classifier of the proposed methodology has a high rate of true positive rate and low false positive rate over other classifiers of existing methods.

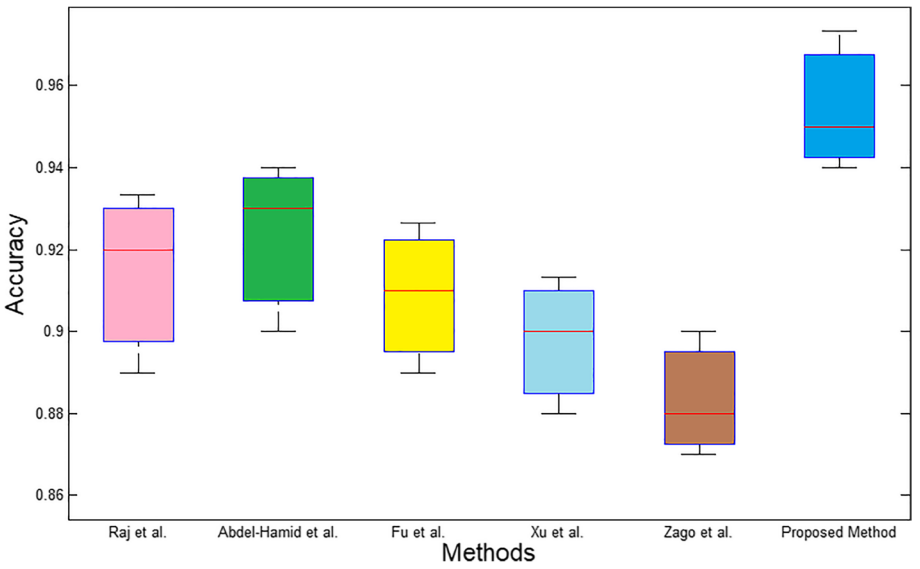

Fig. 10 Comparison of accuracy of different methods

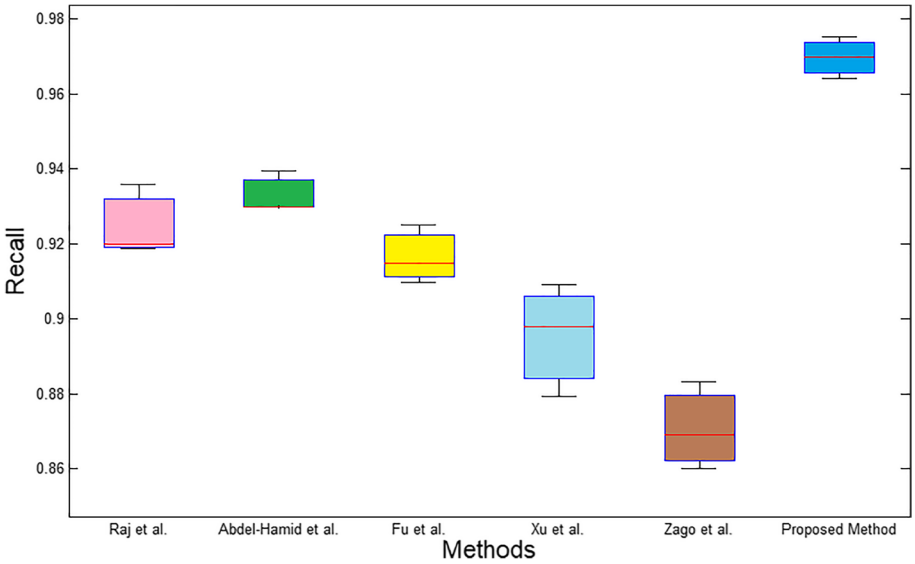

Fig. 11 Comparison of recall parameter of different methods

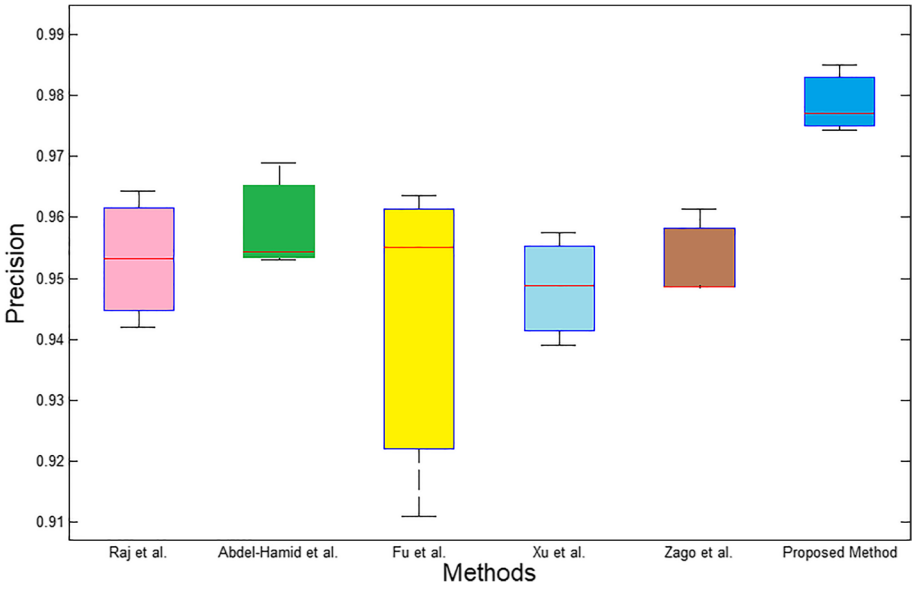

Fig. 12 Comparison of precision parameter of different methods

The confusion matrix of the proposed method and five existing methods, according to the best F-measure, are shown in Fig. 9. From Fig. 9, it is observed that the proposed method's classification grading accuracy has improved. Compared to deep feature-based methods for retinal images, theproposed method achieved superior in classification

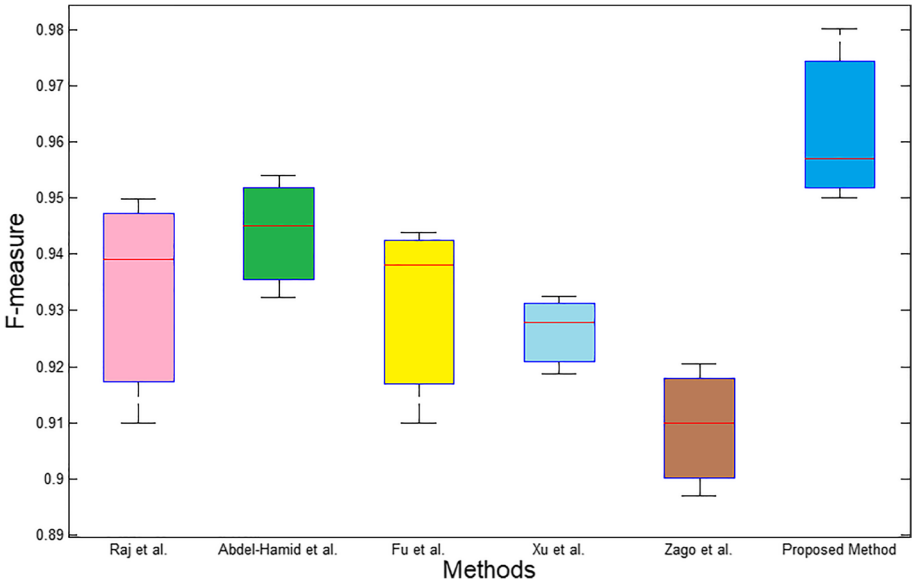

Fig. 13 Comparison of F-measure of different methods

accuracy graded as *eliminate*, which is more significant than graded as *superior* and avoids the wrong classification.

The proposed methodology's enhanced performance is further explained in Figs. 10, 11, 12, and 13. These figures show the range of performance parameters obtained from the existing and proposed methodologies. Methods are represented in horizontal axis and performance results are represented in vertical axis. These figures show the mean performance value for all methods. The accurate predictions of different methods are represented by accuracy is shown in Fig. 10. The correctly predicted true positives for all methods are represented by recall performance in Fig. 11. Figure 12 shows the precision parameter for all methods that predicted the genuine true positives. The accuracy of binary classifier is described through F-measure parameter as shown in Fig. 13 for all methods. These visual representations enrich the understanding of the proposed technique's accuracy regarding robust predictions.

5 Conclusion

The proposed method presented a numeric-based NR-IQA. The proposed method is an improvement over the structured-based NR-IQA methods. A feature-based vector was constructed in this study to analyse and assess image quality. Different features such as NSS, image noise and wavelet distribution parameters were integrated through an SVM classifier. The retinal image was processed through wavelet transform to extract NSS features, including sharpness and contrast. Furthermore, wavelet coefficient modeling was implemented to find the Gaussian noise behaviour in the retinal image as well as the location and signal variance information. Next, the spatial correlations across all sub-bands were analysed by fitting the correlation function. The proposed quality

assessment technique had a higher accuracy than the existing methods. In the future, this method may be used to direct the technician to analyse the enhancement required for automated retinal disease diagnosis applications and may improve the accuracy of diagnosis performance.

Funding The authors state that this work has not received any funding.

Data availability Data sharing not applicable to this article as no datasets were generated or analyzed during the current study.

Declarations

Conflict of interest The authors of this manuscript declare no conflicts of interest.

References

1. Guo T, Liang Z, Gu Y, Liu K, Xu X, Yang J, Yu Q (2023) Learning for retinal image quality assessment with label regularization. Comput Methods Programs Biomed 228:107238
2. Vashist P, Senjam SS, Gupta V, Gupta N, Shamanna BR, Wadhwani M, ..., Bharadwaj A (2022) Blindness and visual impairment and their causes in India: results of a nationally representative survey. PLoS One 17(7):e0271736
3. Sheikh HR, Bovik AC (2006) Image information and visual quality. IEEE Trans Image Process 15(2):430–444
4. Sahu S, Singh HV, Kumar B, Singh AK (2019) De-noising of ultrasound image using Bayesian approached heavy-tailed Cauchy distribution. Multimed Tools Appl 78:4089–4106
5. Abdel-Hamid L, El-Rafei A, Michelson G (2017) No-reference quality index for color retinal images. Comput Biol Med 90:68–75
6. Stępień I, Oszust M (2022) A brief survey on no-reference image quality assessment methods for magnetic resonance images. J Imaging 8(6):160
7. Chow LS, Rajagopal H (2017) Modified-BRISQUE as no reference image quality assessment for structural MR images. Magn Reson Imaging 43:74–87
8. Ou FZ, Wang YG, Zhu G (2019) A novel blind image quality assessment method based on refined natural scene statistics. In: 2019 IEEE international conference on image processing (ICIP). Taipei, Taiwan, pp 1004–1008. https://doi.org/10.1109/ICIP.2019.8803047
9. Niemeijer M, Abramoff MD, van Ginneken B (2006) Image structure clustering for image quality verification of color retina images in diabetic retinopathy screening. Med Image Anal 10(6):888–898
10. MacGillivray TJ, Cameron JR, Zhang Q, El-Medany A, Mulholland C, Sheng Z, ..., UK Biobank Eye and Vision Consortium (2015) Suitability of UK Biobank retinal images for automatic analysis of morphometric properties of the vasculature. PLoS One 10(5):e0127914
11. Xu Z, Zou B, Liu Q (2023) A deep retinal image quality assessment network with salient structure priors. Multimed Tools Appl 82(22):34005–34028. https://doi.org/10.1007/s11042-023-14805-3
12. Raj A, Shah NA, Tiwari AK, Martini MG (2020) Multivariate regression-based convolutional neural network model for fundus image quality assessment. IEEE Access 8:57810–57821
13. Fu H et al (2019) Evaluation of Retinal Image Quality Assessment Networks in Different Color-Spaces. In: Shen D et al (eds) Medical Image Computing and Computer Assisted Intervention – MICCAI 2019. MICCAI 2019. Lecture Notes in Computer Science, vol 11764. Springer, Cham. https://doi.org/10.1007/978-3-030-32239-7_6
14. Wang S, Jin K, Lu H, Cheng C, Ye J, Qian D (2015) Human visual system-based fundus image quality assessment of portable fundus camera photographs. IEEE Trans Med Imaging 35(4):1046–1055
15. Yulianti T, Septama HD, Himayani R, Nugroho HA, Setiawan NA (2022) No reference image quality assessment of retinal image for diabetic retinopathy detection based on feature extraction. AIP conference proceedings, vol 2563. p 080009. https://doi.org/10.1063/5.0103286
16. Nugroho HA, Yulianti T, Setiawan NA, Dharmawan DA (2014) Contrast measurement for no-reference retinal image quality assessment. 2014 6th International Conference on Information Technology and Electrical Engineering (ICITEE), vol 2014. Yogyakarta, Indonesia, pp 1–4. https://doi.org/10.1109/ICITEED.2014.7007902

17. Köhler T, Budai A, Kraus MF, Odstrčilik J, Michelson G, Hornegger J (2013) Automatic no-reference quality assessment for retinal fundus images using vessel segmentation. Proceedings of the 26th IEEE international symposium on computer-based medical systems, vol 2013. Porto, Portugal, pp 95–100. https://doi.org/10.1109/CBMS.2013.6627771
18. Abdel-Hamid L, El-Rafei A, El-Ramly S, Michelson G, Hornegger J (2016) Retinal image quality assessment based on image clarity and content. J Biomed Opt 21(9):096007–096007
19. Zago GT, Andreao RV, Dorizzi B, Salles EOT (2018) Retinal image quality assessment using deep learning. Comput Biol Med 103:64–70
20 Abdel-Hamid L (2021) Retinal image quality assessment using transfer learning: spatial images vs. wavelet detail subbands. Ain Shams Eng J 12(3):2799–2807
21. Hamid LA, El-Rafei A, El-Ramly S, Michelson G, Hornegger J (2015) No-reference wavelet based retinal image quality assessment. In: Computational vision and medical image processing V: proceedings of the 5th eccomas thematic conference on computational vision and medical image processing (VipIMAGE), Spain. pp 123
22. Sahu S, Singh AK (2023) Genetic algorithm based multi-resolution approach for de-speckling OCT image. Multimed Tools Appl 83:1–22. https://doi.org/10.1007/s11042-023-16575-4
23. Jha CK, Kolekar MH (2020) Cardiac arrhythmia classification using tunable Q-wavelet transform based features and support vector machine classifier. Biomed Signal Process Control 59:101875
24. Retina image bank: a project from the American society of Retina specialists. http://imagebank.asrs.org/about. Accessed 30 June 2023
25. König M, Seeböck P, Gerendas BS, Mylonas G, Winklhofer R, Dimakopoulou I, Schmidt-Erfurth UM (2024) Quality assessment of colour fundus and fluorescein angiography images using deep learning. Br J Ophthalmol 108:98–104

Publisher's Note Springer Nature remains neutral with regard to jurisdictional claims in published maps and institutional affiliations.

Springer Nature or its licensor (e.g. a society or other partner) holds exclusive rights to this article under a publishing agreement with the author(s) or other rightsholder(s); author self-archiving of the accepted manuscript version of this article is solely governed by the terms of such publishing agreement and applicable law.